Supporting Information

Magneto-Optical Response and Luminescence Properties of Lanthanide-Titanium-Oxo Clusters Eu_2Ti_7 and Sm_2Ti_7

Wei-Dong Liu, Han Xu, Chong-Yang Li, La-Sheng Long, Lan-Sun Zheng, and Xiang-Jian Kong*

State Key Laboratory of Physical Chemistry of Solid Surfaces, and Department of Chemistry, College of Chemistry and Chemical Engineering, Xiamen University, Xiamen 361005, China

*Corresponding author: **xjkong@xmu.edu.cn**

Physical Measurements

X-ray Crystallography

The crystal data of $\mathbf{Ln_2Ti_7}$ were collected on a Rigaku Oxford Diffraction XtaLAB Synergy diffractometer with micro-focus sealed X-ray Cu-Kα radiation (λ = 1.54184 Å) at 100 K. Crystallography data reduction and faces absorption correction were performed using CrysAlisPro software (Rigaku Oxford Diffraction, 2015). The structures were solved by intrinsic phasing (SHEXT) and refined by full-matrix least-squares calculations based on F^2 using the SHELXTL-2018 software package. All the non-hydrogen atoms were refined anisotropically. The solvent contributions to the scattering factors of $\mathbf{Ln_2Ti_7}$ have been taken into account with PLATON/SQUEEZE. Detailed crystal data and structure refinement parameters for $\mathbf{Ln_2Ti_7}$ are listed in **Table S2** in the Supporting Information.

Photoluminescence Measurement

The excitation and emission spectra of the room-temperature luminescence were measured on the steady-state and transient fluorescence spectrometer (FLS-1000, Edinburgh) equipped with a 450W xenon lamp. The time-resolved PL decay curve was obtained on the same instrument with a microsecond flashlamp. The absolute quantum yield was collected also on the FLS-1000 at room

temperature using a calibrated integrating sphere (coating with a PTFE-like material with a reflectance >99%) as the chamber.

Magnetic Circularly Polarized Luminescence (MCPL) Measurement

The magnetic circularly polarized luminescence spectra were measured on the circularly polarized luminescence pectrometer (CPL-300, JASCO) equipped with a JASCO PM-491 compact permanent magnet (1.6 T) at room temperature. The 1×10^{-3} M CH_2Cl_2 solution of $\mathbf{Eu_2Ti_7}$ was prepared.

Magnetic Circular Dichroism (MCD) Measurement

The magnetic circular dichroism spectra were measured using a JASCO J-1700 equipped with a JASCO PM-491 compact permanent magnet (1.6 T) at room temperature. The 1×10^{-3} M CH_2Cl_2 solution of $\mathbf{Sm_2Ti_7}$ was prepared.

General Instruments

The diffuse reflectance spectra (DRS) were obtained on a UV/Vis/NIR Spectrophotometer (PerkinElmer, Lambda 1050+). Microanalyses of C, H and O elements were carried out with an Element Analyzer (EA, Flash Smart CHNS/O). Thermogravimetric analysis was prepared in N_2 atmosphere using a Thermogravimetric analysis-Mass spectrometry (TGA-MS, SDT-650). The infrared spectra were recorded on an In situ FT-IR Spectrometer (Bruker Vertex 70V) utilizing a single attenuated total reflectance (ATR) accessory. Dynamic light scattering (DLS) analysis was conducted using the laser particle size analyzer (Malvern, ZSU3100). The powder X-ray diffraction (PXRD) pattern was recorded on the Rigaku Smartlab-SE diffractionmeter using Cu-Kα radiation at 25 kV and 100 mA with a scanning rate of 5°/min.

Synthesis, Structure and Characteristic

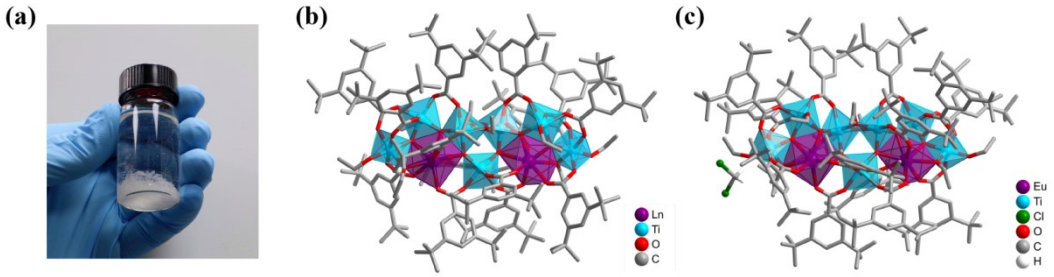

Fig. S1 (a) The physical image of the synthesis result. Crystal structures of (b) $\mathbf{Ln_2Ti_7}$ (Ln = La/Sm/Eu); (c) Recrystallized $\mathbf{Eu_2Ti_7}$.

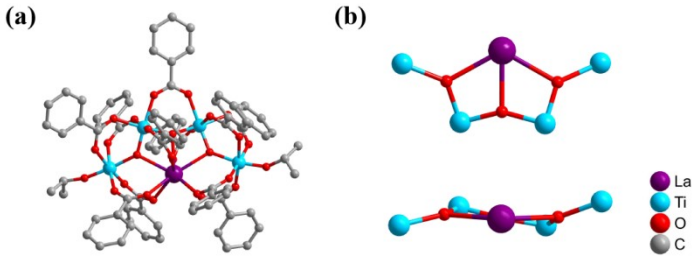

Fig. S2 (a) Crystal structure of $\mathbf{LaTi_4}$. (CCDC: 2082553) (b) Ball-and-stick depiction of metal-oxo core $[LaTi_4(\mu_3\text{-}O)_3]^{13+}$.

Chemicals. In the synthesis process of the used analytically pure lanthanum(III) acetate hydrate ($La(OAc)_3 \cdot xH_2O$), samarium(III) acetate hydrate ($Sm(OAc)_3 \cdot xH_2O$), europium(III) acetate hydrate ($Eu(OAc)_3 \cdot xH_2O$), titanium tetraisopropanolate ($Ti(O^iPr)_4$), 3,5-Di-tert-butylbenzoic acid (HL), ethanol absolute (EtOH) and dichloromethane (CH_2Cl_2) are all the commercial sources and were received without further purification.

Table S1. The information on used chemicals in the synthesis process.

Chemical	CAS	Formula	MW / FW	Brand
Lanthanum Acetate Hydrate ($La(OAc)_3 \cdot xH_2O$)	100587-90-4	$La(OOCCH_3)_3 \cdot xH_2O$	316.04 (MW)	Aladdin
Samarium Acetate Hydrate ($Sm(OAc)_3 \cdot xH_2O$)	100587-91-5	$Sm(OOCCH_3)_3 \cdot xH_2O$	327.49 (MW)	Aladdin
Europium Acetate Hydrate ($Eu(OAc)_3 \cdot xH_2O$)	62667-64-5	$Eu(OOCCH_3)_3 \cdot xH_2O$	329.10 (MW)	Aladdin
Titanium Tetraisopropanolate ($Ti(O^iPr)_4$)	546-68-9	$Ti[OCH(CH_3)_2]_4$	284.23 (FW)	Alfa Aesar
3,5-Di-tert-Butylbenzoic Acid	16225-26-6	$C_{15}H_{22}O_2$	234.33 (MW)	Bidepharm
Ethanol Absolute (EtOH)	64-17-5	C_2H_6O	46.07 (FW)	SCR
Dichloromethane (CH_2Cl_2)	75-09-2	CH_2Cl_2	84.93 (FW)	SCR

Synthesis scheme

$La_2Ti_7(\mu_3\text{-}O)_6(L)_{14}(EtO)_8$ **(La_2Ti_7)**

$La(OAc)_3 \cdot xH_2O$ (63.2 mg, 0.20 mmol), 3,5-Di-tert-butylbenzoic acid (374.9 mg, 1.60 mmol) and 6 mL EtOH were added to an 8 mL vial. Then $Ti(O^iPr)_4$ (180 μL, 0.60 mmol) was added dropwise into the above mixture. The vial was sealed and sonicated for 20 min. Colorless block-shaped crystals were obtained after 2 days in a 80 °C temperature environment (36.7% yield based on $La(OAc)_3 \cdot xH_2O$). Anal. Calcd for $C_{226}H_{334}O_{42}La_2Ti_7$ (FW = 4336.03): C, 62.60; H, 7.75; O, 15.50 (%); Found: C, 62.57; H, 7.78; O, 15.61 (%).

$Sm_2Ti_7(\mu_3\text{-}O)_6(L)_{14}(EtO)_8$ **(Sm_2Ti_7)**

$Sm(OAc)_3 \cdot xH_2O$ (98.2 mg, 0.30 mmol), 3,5-Di-tert-butylbenzoic acid (468.7 mg, 2.00 mmol) and 7 mL EtOH were added to an 8 mL vial. Then $Ti(O^iPr)_4$ (165 μL, 0.55 mmol) was added dropwise into the above mixture. The vial was sealed and sonicated for 5 min. Colorless block-shaped crystals were obtained after 1 day in a 80 °C temperature environment (42.6% yield based on $Sm(OAc)_3 \cdot xH_2O$). Anal. Calcd for $C_{226}H_{334}O_{42}Sm_2Ti_7$ (FW = 4358.91): C, 62.27; H, 7.71; O, 15.42 (%); Found: C, 62.32; H, 7.74; O, 15.36 (%).

$Eu_2Ti_7(\mu_3\text{-}O)_6(L)_{14}(EtO)_8$ **(Eu_2Ti_7)**

Eu_2Ti_7 was synthesized by the same method nothing but the substitution of $Sm(OAc)_3 \cdot xH_2O$ (98.2 mg, 0.30 mmol) to $Eu(OAc)_3 \cdot xH_2O$ (98.7 mg, 0.30 mmol). Colorless block-shaped crystals were obtained after 1 day in a 80 °C temperature environment (45.8% yield based on $Eu(OAc)_3 \cdot xH_2O$). Anal. Calcd for $C_{226}H_{334}O_{42}Eu_2Ti_7$ (FW = 4362.13): C, 62.22; H, 7.70; O, 15.41 (%); Found: C, 62.26; H, 7.74; O, 15.31 (%).

$Eu_2Ti_7(\mu_3\text{-}O)_6(L)_{14}(EtO)_8 \cdot CH_2Cl_2$ (Recrystallized **Eu_2Ti_7**)

The **Eu_2Ti_7** sample synthesized by the solvothermal method was dissolved in dichloromethane to obtain a clarified solution. After the slow evaporation of the solvent, new colorless block-shaped crystals were formed (12.3% yield based on **Eu_2Ti_7**). Anal. Calcd for $C_{227}H_{336}O_{42}Cl_2Eu_2Ti_7$ (FW = 4447.06): C, 61.30; H, 7.60; O, 15.11 (%); Found: C, 61.35; H, 7.68; O, 15.25 (%).

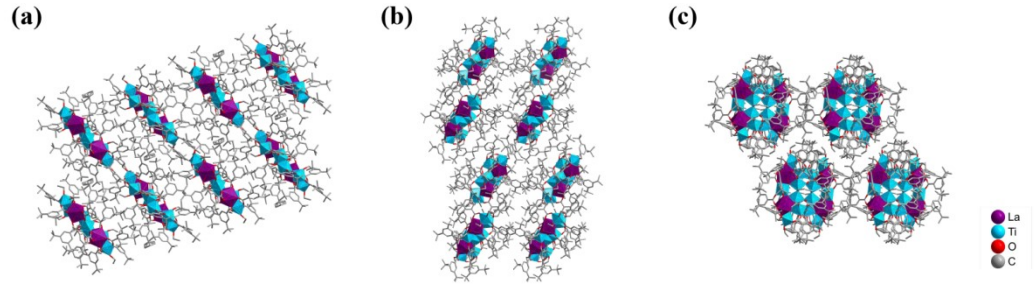

Fig. S3 The packing structures of $\mathbf{La_2Ti_7}$ in (a) a-axis, (b) b-axis and (c) c-axis.

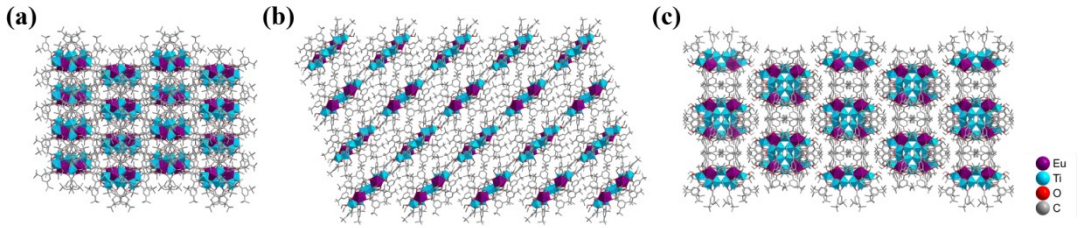

Fig. S4 The packing structures of $\mathbf{Sm_2Ti_7}$ in (a) a-axis, (b) b-axis and (c) c-axis.

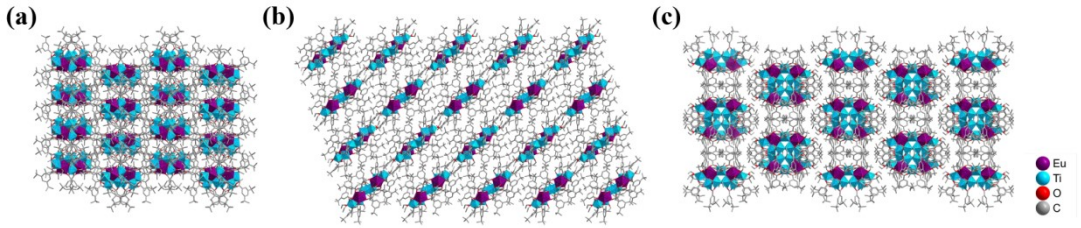

Fig. S5 The packing structures of $\mathbf{Eu_2Ti_7}$ in (a) a-axis, (b) b-axis and (c) c-axis.

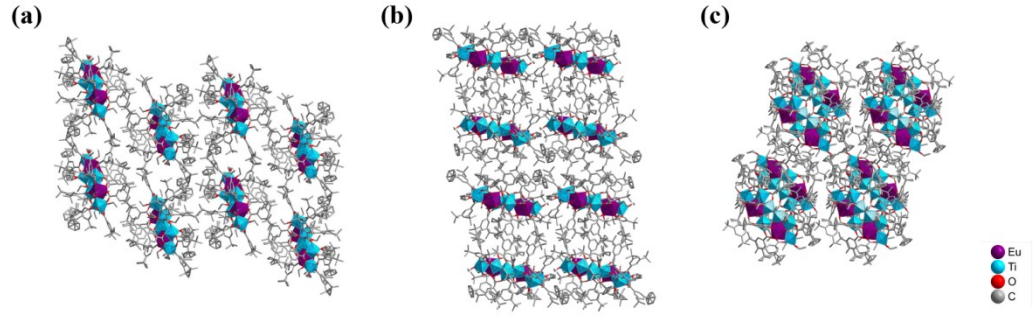

Fig. S6 The packing structures of recrystallized $\mathbf{Eu_2Ti_7}$ in (a) a-axis, (b) b-axis and (c) c-axis.

Table S2. Single crystal structure refinements of **Ln_2Ti_7**.

Ln_2Ti_7	**La_2Ti_7**	**Sm_2Ti_7**	**Eu_2Ti_7**	Recrystallized **Eu_2Ti_7**
CCDC	2392364	2392362	2392363	2392375
Empirical formula	$C_{226}H_{334}O_{42}La_2Ti_7$	$C_{226}H_{334}O_{42}Sm_2Ti_7$	$C_{226}H_{334}O_{42}Eu_2Ti_7$	$C_{227}H_{336}O_{42}Cl_2Eu_2Ti_7$
Formula weight	4336.03	4358.91	4362.13	4447.06
Temperature/K	100.0(10)	100.01(10)	100.00(10)	106(6)
Crystal color	colorless	colorless	colorless	colorless
Crystal system	triclinic	triclinic	monoclinic	triclinic
Space group	*P*-1	*P*-1	*C*2/*c*	*P*-1
a/Å	20.7274(5)	20.7017(8)	40.1910(13)	20.1724(2)
b/Å	22.4287(5)	22.2762(8)	20.5124(5)	21.9592(2)
c/Å	31.2329(6)	31.0854(9)	31.0940(11)	31.4923(3)
α/°	73.684(2)	72.953(3)	90	95.7290(10)
β/°	87.696(2)	87.194(3)	106.338(4)	93.4250(10)
γ/°	62.609(2)	63.073(4)	90	109.2320(10)
V/Å^3	12305.0(5)	12160.3(9)	24599.2(14)	13042.0(2)
Z	2	2	4	2
ρ_{calc}/g·cm^{-3}	1.170	1.190	1.178	1.132
μ/mm^{-1}	4.961	5.931	5.929	5.784
2*θ* range/°	4.646 - 110.76	4.67 - 103.282	5.929 - 130.152	4.296 - 154.716
Reflections collected	92912	79692	58644	180196
Data/restraints/parameters	30704/2912/2365	26124/3086/2438	20235/1354/1195	52642/3846/3054
Goodness-of-fit on F^2	1.027	1.028	1.010	1.053
Final R indexes [I>=2σ (I)] [a]	R_1 = 0.1160, wR_2 = 0.2991	R_1 = 0.1156, wR_2 = 0.3034	R_1 = 0.1261, wR_2 = 0.3288	R_1 = 0.0673, wR_2 = 0.1840
Final R indexes [all data] [b]	R_1 = 0.1896, wR_2 = 0.3457	R_1 = 0.2042, wR_2 = 0.3564	R_1 = 0.1780, wR_2 = 0.3688	R_1 = 0.0822, wR_2 = 0.1955

[a] $R_1 = \sum(\, | |F_o| - |F_c| \, |) \, / \sum |F_o|$; [b] $wR_2 = \{\sum [w \, (F_o^2 - F_c^2)^2] \, / \sum [w(F_o^2)^2]\}^{1/2}$;

$w = 1/[^2(F_o)^2+(aP)^2+bP]$ and $P = (F_o^2+2F_c^2)/3$.

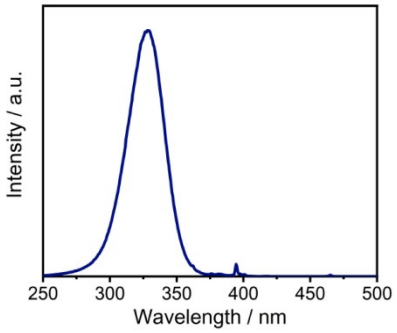

Fig. S7 Excitation spectrum of the CH_2Cl_2 solution of **Eu_2Ti_7** with concentration 1×10^{-3} M.

Table S3. The prominent g_{lum} and g_{MCPL} values versus wavelengths in MCPL of **Eu_2Ti_7**.

f-f transition	Wavelength / nm	g_{lum} (1.6 T)		g_{MCPL} (T^{-1})	
		N→S	S→N	N→S	S→N
$^5D_0\rightarrow{}^7F_1$	586	0.0236	-0.0226	0.0148	-0.0141
	599	-0.0219	0.0212	-0.0137	0.0133
$^5D_0\rightarrow{}^7F_2$	612	-0.0121	0.0103	-0.0076	0.0064
	625	0.0130	-0.0123	0.0081	-0.0077
$^5D_0\rightarrow{}^7F_4$	695	-0.0402	0.0353	-0.0251	0.0221
	709	0.0610	-0.0634	0.0381	-0.0396

Calculates g_{lum} and Delta I from the CPL signal (y-axis is CD [mdeg]) and DC signal (y-axis is DC [V]). This calculation uses an equation to convert the CPL signal. Note: Use this function only for CPL data obtained using the CPL instruments.

Delta I = CD [mdeg] × 0.000069813

g_{lum} = ΔI / I = CD [mdeg] ÷ DC [V] × 0.000069813

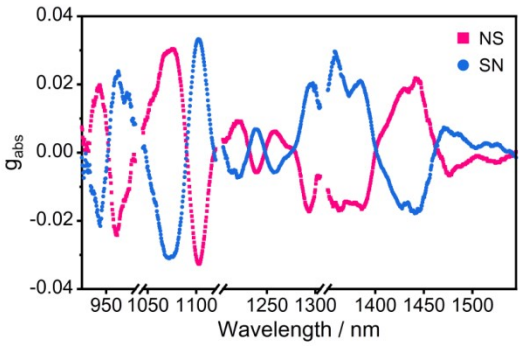

Fig. S8 Correspondence between g_{abs} value and wavelength in MCD of **Sm_2Ti_7**.

Table S4. The prominent g_{abs} and g_{MCD} values versus wavelengths in MCD of **Sm_2Ti_7**.

f-f transition	Wavelength / nm	g_{abs} (1.6 T)		g_{MCD} (T^{-1})	
		N→S	S→N	N→S	S→N
$^6H_{5/2}\rightarrow{}^6F_{11/2}$	944	0.0198	-0.0216	0.0124	-0.0135
	962	-0.0242	0.0239	-0.0151	0.0149
$^6H_{5/2}\rightarrow{}^6F_{9/2}$	1076	0.0304	-0.0310	0.0190	-0.0194
	1102	-0.0327	0.0332	-0.0204	0.0208
$^6H_{5/2}\rightarrow{}^6F_{7/2}$	1220	0.0093	-0.0074	0.0058	-0.0046
	1239	-0.0058	0.0068	-0.0036	0.0043
	1257	0.0062	-0.0058	0.0039	-0.0036
$^6H_{5/2}\rightarrow{}^6F_{5/2}$	1296	-0.0173	0.0201	-0.0108	0.0126
	1360	-0.0160	0.0296	-0.0100	0.0185
	1385	-0.0166	0.0211	-0.0104	0.0132
$^6H_{5/2}\rightarrow{}^6F_{3/2}$	1442	0.0219	-0.0175	0.0137	-0.0109
$^6H_{5/2}\rightarrow{}^6F_{1/2}$	1476	-0.0068	0.0074	-0.0043	0.0046

Calculates g_{abs} and Delta A from the CD signal (y-axis is CD [mdeg]) and Abs signal. This calculation uses an equation to convert the CD signal. Note: Use this function only for CD data obtained using the CD instruments.

Delta A = CD [mdeg] / 32982

g_{abs} = ΔA / A = (CD [mdeg] / 32982) ÷ Abs

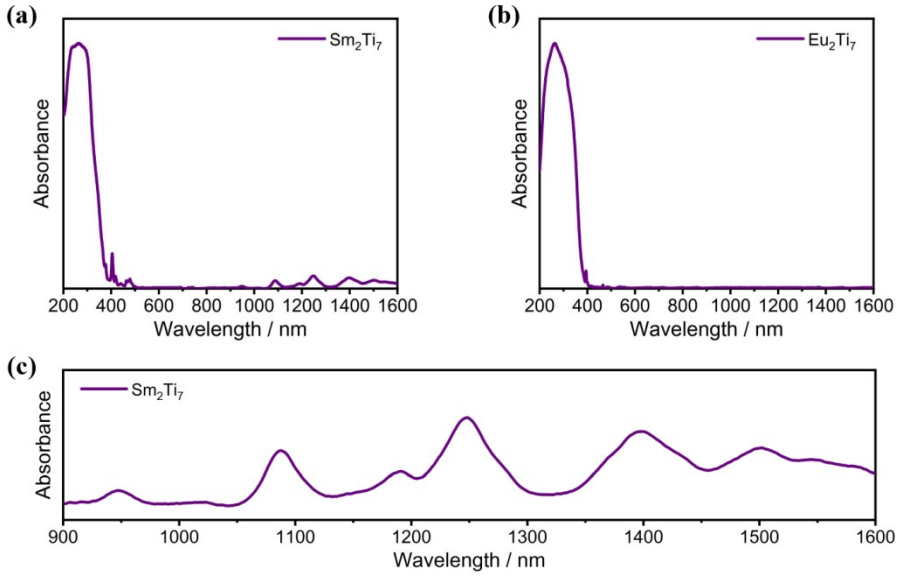

Fig. S9 (a) & (c) The solid diffuse reflectance spectra (DRS) of **Sm_2Ti_7** from 200 to 1600 nm and 900 to 1600 nm; (b) The solid DRS of **Eu_2Ti_7** from 200 to 1600 nm.

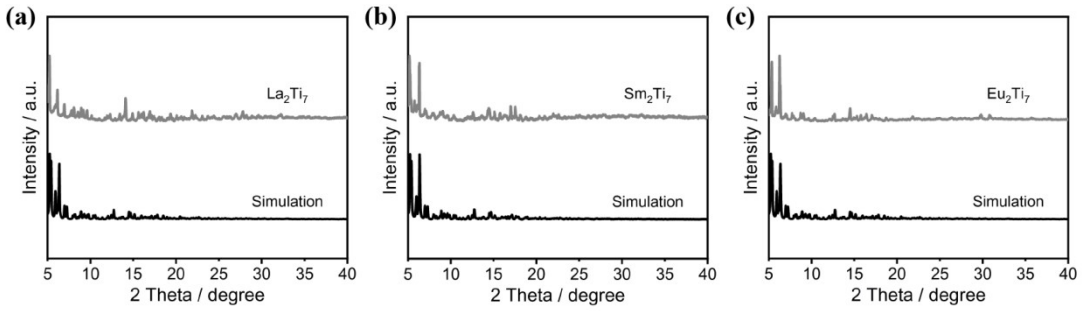

Fig. S10 The powder X-ray diffraction (PXRD) of **Ln_2Ti_7**: Ln = (a) La; (b) Sm; (c) Eu.

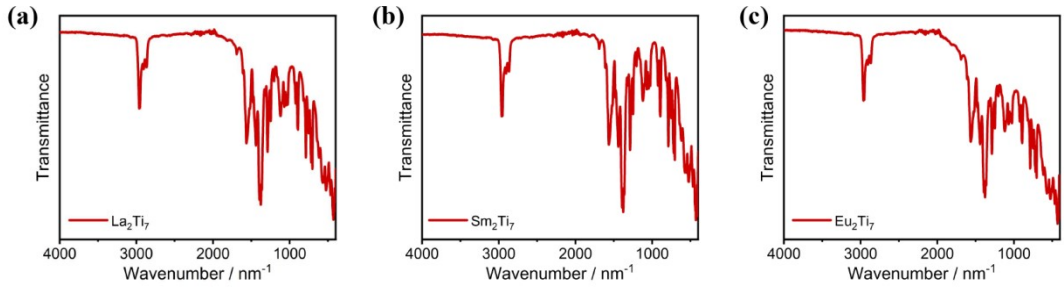

Fig. S11 The fourier transform infrared (FT-IR) spectra of $\mathbf{Ln_2Ti_7}$: Ln = (a) La; (b) Sm; (c) Eu.

The FT-IR spectra of $\mathbf{Ln_2Ti_7}$ have similar peak shapes. $\mathbf{La_2Ti_7}$ FT-IR (cm^{-1}): 2960 (s), 2905 (m), 2868 (m), 1690 (w), 1609 (s), 1564 (s), 1476 (s), 1439 (s), 1392 (vs), 1378 (vs), 1361 (vs), 1316 (s), 1287 (s), 1247 (s), 1200 (m), 1118 (s), 1068 (s), 1043 (s), 1025 (s), 921 (s), 892 (s), 820 (s), 786 (s), 751 (s), 718 (s), 703 (s), 614 (s), 569 (s), 549 (s), 524 (s), 466 (s), 429 (vs). $\mathbf{Sm_2Ti_7}$ FT-IR (cm^{-1}): 2961 (s), 2904 (m), 2867 (m), 1691 (w), 1609 (s), 1564 (s), 1477 (s), 1441 (s), 1391 (vs), 1378 (vs), 1361 (vs), 1316 (s), 1288 (s), 1246 (s), 1201 (m), 1118 (s), 1068 (s), 1042 (s), 1026 (s), 922 (s), 892 (s), 818 (s), 787 (s), 751 (s), 718 (s), 703 (s), 616 (s), 569 (s), 548 (s), 524 (s), 466 (s), 429 (vs), 407 (vs). $\mathbf{Eu_2Ti_7}$ FT-IR (cm^{-1}): 2960 (s), 2904 (m), 2866 (m), 1691 (w), 1609 (s), 1564 (s), 1478 (s), 1441 (s), 1391 (vs), 1378 (vs), 1361 (vs), 1316 (s), 1288 (s), 1246 (s), 1201 (m), 1118 (s), 1068 (s), 1040 (s), 1026 (s), 921 (s), 891 (s), 819 (s), 787 (s), 750 (s), 718 (s), 703 (s), 616 (s), 569 (s), 548 (s), 524 (s), 466 (s), 429 (vs), 404 (vs). $\mathbf{La_2Ti_7}$ is taken as an example for analysis. The absorptions at 2960 cm^{-1}, 2905 cm^{-1}, and 2868 cm^{-1} are due to the C-H stretching vibrations of $-CH_3$ and $-CH_2-$ on the carboxylic acid ligands and EtO^-. The absorption at ~1250 cm^{-1} belongs to the bending vibration of $-C(CH_3)_3$ of the carboxylic acid ligands. In addition, the absorptions of the skeletal vibrations of the benzene ring of the carboxylic acid ligands are in the range of 1650-1450 cm^{-1}, the absorptions of the C-H stretching vibrations are at ~3000 cm^{-1}, and the absorptions of the C-H bending vibrations are in the range of 910-650 cm^{-1}. The absorptions at ~1400 cm^{-1} and 1610-1500 cm^{-1} are attributed to the symmetric and antisymmetric stretching vibrations of the carbonyl C=O after the carboxylic acid ligands are deprotonated, and both are relatively strong absorptions. The other absorption peaks in the band of 1060 cm^{-1} to 400 cm^{-1} are mainly attributed to the metal-oxygen vibrations.

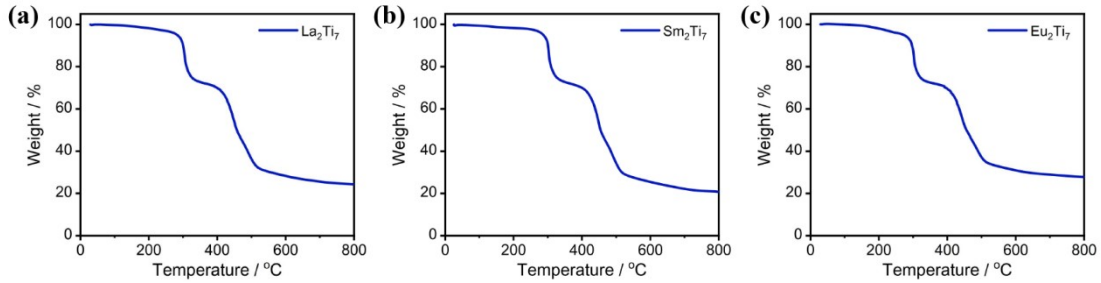

Fig. S12 The thermo gravimetric analysis (TGA) curves of $\mathbf{Ln_2Ti_7}$: Ln = (a) La; (b) Sm; (c) Eu.

The TGA curves of $\mathbf{Ln_2Ti_7}$ have similar shapes and trends. The weight loss rates of $\mathbf{La_2Ti_7/Sm_2Ti_7/Eu_2Ti_7}$ in the range of room temperature to 280 °C are 4.7%, 3.8% and 5.1% respectively, which are due to the departure of solvent molecules. The curves of $\mathbf{Ln_2Ti_7}$ drop sharply between 280 and 320 °C with weight loss of approximately 25%, indicating the initial decomposition of carboxylic acid ligands. From 320 and 400 °C, the weight loss rate slows down, though additional loss of around 5% occurs. Between 400 and 520 °C, $\mathbf{Ln_2Ti_7}$ begins to disintegrate completely, and the curves show a significant drop, which is attributed to the complete decomposition of carboxylic acid ligands and the collapse of the metal-oxo frameworks. When the temperature is higher than 520 °C, the curves remain basically stable, and at this time the samples mainly exist in the form of metal oxides. The final residual weights for $\mathbf{La_2Ti_7/Sm_2Ti_7/Eu_2Ti_7}$ are 24.2%, 23.1% and 27.8% respectively.

Table S5. Selected bond distances (Å) of La_2Ti_7.

Atom-Atom	Length/Å	Atom-Atom	Length/Å
La1—O8	2.523 (8)	La2—O1	2.451 (9)
La1—O22	2.464 (10)	La2—O16	2.611 (9)
La1—O24	2.495 (10)	La2—O20	2.515 (9)
La1—O36	2.490 (10)	La2—O3	2.518 (12)
La1—O40	2.447 (9)	La2—O25	2.510 (9)
La1—O13	2.559 (8)	La2—O2	2.464 (12)
La1—O7	2.522 (9)	La2—O35	2.467 (10)
La1—O29	2.583 (9)	La2—O9	2.542 (13)
Ti1—O12	1.989 (10)	Ti7—O6	1.995 (10)
Ti1—O16	1.803 (8)	Ti7—O14	2.068 (10)
Ti1—O28	2.134 (9)	Ti7—O16	1.927 (8)
Ti1—O42	1.975 (9)	Ti7—O20	1.807 (9)
Ti1—O13	1.820 (10)	Ti7—O32	1.926 (9)
Ti1—O19	2.064 (14)	Ti7—O34	2.025 (9)
Ti4—O4	2.041 (11)	Ti2—O8	1.952 (10)
Ti4—O8	1.755 (9)	Ti2—O26	2.089 (12)
Ti4—O14	1.947 (9)	Ti2—O40	1.822 (9)
Ti4—O18	1.984 (9)	Ti2—O15	2.065 (12)
Ti4—O32	2.077 (9)	Ti2—O33	2.057 (11)
Ti4—O13	1.902 (9)	Ti2—O37	1.799 (11)
Ti6—O1	1.832 (10)	Ti5—O30	2.019 (13)
Ti6—O10	2.101 (10)	Ti5—O40	1.969 (9)
Ti6—O20	1.903 (9)	Ti5—O11	1.805 (11)
Ti6—O38	2.105 (11)	Ti5—O27	2.068 (13)
Ti6—O21	1.781 (10)	Ti5—O29	1.858 (10)
Ti6—O23	2.067 (11)	Ti5—O17	2.102 (11)
Ti3—O1	1.953 (10)	Ti3—O39	1.810 (12)
Ti3—O31	1.989 (11)	Ti3—O5	1.992 (12)
Ti3—O9	1.851 (13)	Ti3—O41	2.103 (13)

Table S6. Selected bond angles (°) of La_2Ti_7.

Ti6-O1-La2	107.7(4)	Ti6-O20-La2	103.0(4)
Ti6-O1-Ti3	133.0(4)	Ti7-O20-La2	106.6(4)
Ti3-O1-La2	107.0(4)	Ti7-O20-Ti6	146.0(5)
Ti4-O8-La1	108.0(4)	Ti2-O40-La1	109.3(4)
Ti4-O8-Ti2	144.9(6)	Ti2-O40-Ti5	131.7(6)

Ti2-O8-La1	102.2(4)	Ti5-O40-La1	105.7(3)
Ti1-O16-La2	119.0(4)	Ti1-O13-La1	116.0(4)
Ti1-O16-Ti7	137.2(6)	Ti1-O13-Ti4	138.1(5)
Ti7-O16-La2	99.4(3)	Ti4-O13-La1	102.0(4)

Table S7. Selected bond distances (Å) of **Sm_2Ti_7**.

Sm1—O8	2.529 (10)	Sm2—O20	2.423 (10)
Sm1—O10	2.350 (11)	Sm2—O30	2.532 (11)
Sm1—O12	2.420 (9)	Sm2—O32	2.359 (11)
Sm1—O16	2.526 (10)	Sm2—O11	2.413 (12)
Sm1—O34	2.385 (12)	Sm2—O23	2.330 (13)
Sm1—O36	2.453 (10)	Sm2—O25	2.396 (12)
Sm1—O7	2.402 (11)	Sm2—O13	2.440 (13)
Sm1—O33	2.392 (11)	Sm2—O37	2.528 (12)
Ti1—O1	1.978 (10)	Ti7—O10	1.881 (11)
Ti1—O6	2.056 (12)	Ti7—O12	1.960 (11)
Ti1—O8	1.903 (9)	Ti7—O26	2.107 (14)
Ti1—O12	1.756 (11)	Ti7—O28	2.080 (14)
Ti1—O38	1.972 (11)	Ti7—O29	1.792 (14)
Ti1—O42	2.051 (12)	Ti7—O15	2.077 (12)
Ti4—O4	1.983 (13)	Ti2—O10	1.893 (11)
Ti4—O8	1.834 (10)	Ti2—O14	2.023 (13)
Ti4—O30	1.836 (10)	Ti2—O16	1.859 (12)
Ti4—O40	1.961 (14)	Ti2—O3	2.109 (14)
Ti4—O27	2.125 (11)	Ti2—O2	2.006 (14)
Ti4—O41	2.056 (13)	Ti2—O19	1.861 (13)
Ti6—O1	2.069 (12)	Ti5—O20	1.868 (11)
Ti6—O6	1.983 (11)	Ti5—O22	2.074 (13)
Ti6—O18	2.096 (11)	Ti5—O32	1.852 (11)
Ti6—O20	1.833 (11)	Ti5—O21	2.074 (13)
Ti6—O24	1.995 (11)	Ti5—O31	2.083 (14)
Ti6—O30	1.917 (11)	Ti5—O35	1.769 (15)
Ti3—O32	1.939 (12)	Ti3—O37	1.929 (15)
Ti3—O17	1.982 (15)	Ti3—O39	2.005 (14)
Ti3—O9	2.089 (15)	Ti3—O5	1.783 (15)

Table S8. Selected bond angles (°) of **Sm_2Ti_7**.

Ti1-O8-Sm1	99.4(4)	Ti6-O20-Sm2	105.6(5)

Ti4-O8-Sm1	117.5(4)	Ti6-O20-Ti5	146.5(6)
Ti4-O8-Ti1	137.3(5)	Ti5-O20-Sm2	103.8(5)
Ti7-O10-Sm1	107.5(5)	Ti4-O30-Sm2	121.6(5)
Ti7-O10-Ti2	130.9(5)	Ti4-O30-Ti6	134.4(6)
Ti2-O10-Sm1	108.6(5)	Ti6-O30-Sm2	99.0(4)
Ti1-O12-Sm1	108.1(5)	Ti5-O32-Sm2	106.7(5)
Ti1-O12-Ti7	146.1(6)	Ti5-O32-Ti3	133.4(6)
Ti7-O12-Sm1	102.3(4)	Ti3-O32-Sm2	107.4(5)

Table S9. Selected bond distances (Å) of **Eu_2Ti_7**.

Eu1—O1	2.507 (7)	Ti1—O1	1.842 (7)
Eu1—O10	2.394 (7)	Ti1—O6	1.981 (7)
Eu1—O12	2.404 (8)	Ti1—O7	2.055 (9)
Eu1—O14	2.302 (8)	Ti4—O1	1.914 (7)
Eu1—O16	2.353 (8)	Ti4—O4	1.943 (7)
Eu1—O20	2.424 (9)	Ti4—O8	2.001 (7)
Eu1—O21	2.389 (8)	Ti4—O10	1.790 (8)
Eu1—O13	2.524 (10)	Ti4—O18	2.054 (8)
Ti2—O10	1.927 (7)	Ti3—O14	1.975 (9)
Ti2—O14	1.857 (9)	Ti3—O13	1.907 (11)
Ti2—O11	2.102 (11)	Ti3—O2	2.021 (12)
Ti2—O3	1.787 (9)	Ti3—O17	2.042 (13)
Ti2—O15	2.113 (9)	Ti3—O9	2.068 (12)
Ti2—O19	1.986 (11)	Ti3—O5	1.787 (12)

Table S10. Selected bond angles (°) of **Eu_2Ti_7**.

Ti1-O1-Eu1	121.0(3)	Ti4-O10-Eu1	108.0(3)
Ti1-O1-Ti4	134.1(4)	Ti4-O10-Ti2	143.4(4)
Ti4-O1-Eu1	99.8(3)	Ti2-O10-Eu1	103.6(3)
Ti2-O14-Eu1	109.6(4)	Ti3-O14-Eu1	107.4(4)
Ti2-O14-Ti3	129.4(4)		

Table S11. Selected bond distances (Å) of recrystallized **Eu_2Ti_7**.

Eu1—O8	2.397 (3)	Eu2—O24	2.388 (3)
Eu1—O22	2.351 (3)	Eu2—O26	2.382 (3)
Eu1—O30	2.577 (3)	Eu2—O32	2.387 (3)
Eu1—O34	2.364 (3)	Eu2—O40	2.409 (3)

Eu1—O23	2.333 (3)	Eu2—O3	2.530 (3)
Eu1—O27	2.327 (3)	Eu2—O13	2.355 (3)
Eu1—O2	2.452 (3)	Eu2—O7	2.363 (3)
Eu1—O33	2.459 (3)	Eu2—O39	2.497 (3)
Ti1—O1	2.058 (3)	Ti7—O18	1.994 (3)
Ti1—O4	1.951 (3)	Ti7—O30	1.810 (3)
Ti1—O6	2.000 (3)	Ti7—O43	2.053 (3)
Ti1—O8	1.781 (3)	Ti7—O3	1.840 (3)
Ti1—O14	2.053 (3)	Ti7—O17	1.980 (3)
Ti1—O30	1.922 (3)	Ti7—O37	2.070 (3)
Ti4—O8	1.946 (3)	Ti2—O10	2.080 (3)
Ti4—O22	1.822 (3)	Ti2—O20	2.079 (3)
Ti4—O36	2.112 (3)	Ti2—O24	1.931 (3)
Ti4—O25	2.043 (3)	Ti2—O26	1.833 (3)
Ti4—O29	2.040 (3)	Ti2—O35	2.047 (3)
Ti4—O31	1.792 (3)	Ti2—O19	1.791 (4)
Ti6—O1	1.954 (3)	Ti5—O12	2.041 (3)
Ti6—O4	2.049 (3)	Ti5—O22	1.940 (3)
Ti6—O16	1.998 (3)	Ti5—O28	1.979 (3)
Ti6—O24	1.781 (3)	Ti5—O38	2.080 (3)
Ti6—O3	1.903 (3)	Ti5—O42	1.804 (3)
Ti6—O15	2.047 (3)	Ti5—O33	1.877 (3)
Ti3—O26	1.932 (3)	Ti3—O39	1.879 (4)
Ti3—O11	2.040 (3)	Ti3—O5	2.015 (4)
Ti3—O9	2.089 (4)	Ti3—O41	1.829 (4)

Table S12. Selected bond angles (°) of recrystallized **Eu_2Ti_7**.

Ti1-O8-Eu1	107.55(12)	Ti2-O26-Eu2	107.30(12)
Ti1-O8-Ti4	144.85(16)	Ti2-O26-Ti3	132.43(17)
Ti4-O8-Eu1	102.91(11)	Ti3-O26-Eu2	105.52(14)
Ti4-O22-Eu1	108.86(12)	Ti1-O30-Eu1	96.68(10)
Ti4-O22-Ti5	133.30(15)	Ti7-O30-Eu1	124.51(13)
Ti5-O22-Eu1	106.03(13)	Ti7-O30-Ti1	135.73(16)
Ti6-O24-Eu2	106.38(13)	Ti6-O3-Eu2	97.48(11)
Ti6-O24-Ti2	147.63(17)	Ti7-O3-Eu2	120.16(13)
Ti2-O24-Eu2	103.78(11)	Ti7-O3-Ti6	136.03(15)